Biochemical and Biophysical Research Communications 451 (2014) 562–567

Contents lists available at ScienceDirect

Biochemical and Biophysical Research Communications

journal homepage: www.elsevier.com/locate/ybbrc

Expression and localization of aquaporin-4 in sensory ganglia

Jungo Kato [a,b,1], Yoshiki Takai [c], Mariko Kato Hayashi [a], Yasuhiro Kato [a], Manami Tanaka [a], Yoshiro Sohma [a], Yoichiro Abe [a], Masato Yasui [a,*]

[a] Department of Pharmacology, Keio University School of Medicine, 35 Shinanomachi, Shinjuku, Tokyo 160-8582, Japan
[b] Department of Anesthesiology, Keio University School of Medicine, 35 Shinanomachi, Shinjuku, Tokyo 160-8582, Japan
[c] Department of Neurology, Tohoku University School of Medicine, 1-1 Seiryo-cho, Aoba-ku, Sendai, Miyagi 980-8574, Japan

ARTICLE INFO

Article history:
Received 11 July 2014
Available online 12 August 2014

Keywords:
AQP4
The peripheral nervous system
Sensory ganglia
Satellite glial cells
Water homeostasis

ABSTRACT

Aquaporin-4 (AQP4) is a water channel protein that is predominantly expressed in astrocytes in the CNS. The rapid water flux through AQP4 may contribute to electrolyte/water homeostasis and may support neuronal activities in the CNS. On the other hand, little is known about the expression of AQP4 in the peripheral nervous system (PNS). Using AQP4$^{-/-}$ mice as a negative control, we demonstrated that AQP4 is also expressed in sensory ganglia, such as trigeminal ganglia and dorsal root ganglia in the PNS. Immunohistochemistry revealed that AQP4 is exclusively localized to satellite glial cells (SGCs) surrounding the cell bodies of the primary afferent sensory neurons in the sensory ganglia. Biochemical analyses revealed that the expression levels of AQP4 in sensory ganglia were considerably lower than those in astrocytes in the CNS. Consistently, behavioral analyses did not show any significant difference in terms of mechanical and cold sensitivity between wild type and AQP4$^{-/-}$ mice. Overall, although the pathophysiological relevance of AQP4 in somatosensory perception remains unclear, our findings provide new insight into the involvement of water homeostasis in the peripheral sensory system.

1. Introduction

Aquaporin-4 (AQP4), a water channel protein, is widely expressed in various organs including the central nervous system (CNS), kidney, intestine, skeletal muscle, lung and secretory glands [1–3]. AQP4 forms stable tetramers in plasma membranes; in these tetramers, each monomer contains six transmembrane helical domains with two shorter helical segments, forming a narrow water-selective pore [4]. Structural studies and molecular dynamic simulations suggest that steric and electrostatic factors contribute to AQP4's highly efficient and selective ability to transport water [5,6].

In the CNS, AQP4 is exclusively expressed in astrocytes. AQP4 localizes specifically at foot processes extending toward brain–water interfaces, such as vascular endfeet and the glia limitans [7,8]. Given this polarization, AQP4 is thought to play an important role in brain–water homeostasis. Moreover, recent studies have shown the involvement of water flux through AQP4 in neuronal activities in the CNS. AQP4$^{-/-}$ mice exhibit abnormalities in the electrophysiological activities of their neurons, such as altered sensory-evoked potentials and increased seizure duration [9–12]. Although the underlying mechanism remains unclear, AQP4-dependent water permeation is thought to play an important role in K^+ reuptake by astrocytes following neuronal excitation, contributing to electrolyte/water homeostasis in the extracellular space for the securement of normal neuronal activities. Therefore, AQP4 is now considered to be a potential therapeutic target for various neurological disorders that involve the abnormal water/electrolyte homeostasis, such as brain edema and epilepsy. Previously, we demonstrated that propofol, a general anesthetic drug, profoundly inhibits the osmotic water permeability of AQP4 in the presence of Zn^{2+} [13].

On the other hand, little attention has been given to the expression and function of AQP4 in the peripheral nervous system (PNS). Descriptions of AQP4 expression in the PNS have only been made for neurons in the enteric nerve plexus [14,15]. Sensory ganglia, which consist of small nodular structures connecting to the spinal cord and brain, contain the cell bodies of primary afferent neurons that convey sensory input from the periphery to the CNS [16]. In sensory ganglia, the neuronal cell bodies are thoroughly wrapped by non-neuronal cells called satellite glial cells (SGCs). Similar to astrocytes in the CNS, SGCs also express various kinds of ion channels and transporters and contribute to the regulation of the

* Corresponding author. Fax: +81 3 3359 8889.
E-mail address: myasui@a3.keio.jp (M. Yasui).
[1] Present address: Department of Physiology and Pharmacology, Karolinska Institutet, Von Eulers väg 8, 171 77 Stockholm, Sweden.

http://dx.doi.org/10.1016/j.bbrc.2014.08.026
0006-291X/

extracellular space (ECS) around the neurons, which is the reason why SGCs are often described as peripheral astrocytes [17]. Given the great functional similarities between astrocytes and SGCs, it seems reasonable that SGCs might also express AQP4.

In this study, we examined the expression of AQP4 in sensory ganglia, including dorsal root ganglia (DRG) and trigeminal ganglia (TG), using AQP4$^{-/-}$ mice as negative controls and sought to explore the potential roles of AQP4 in peripheral somatosensory perception.

2. Materials and methods

2.1. Animals

All animal procedures were performed with an approved protocol from the Animal Care Committee of Keio University School of Medicine, in accordance with the Guidelines for Proper Conduct of Animal Experiment and Related Academic Research Institutions under the jurisdiction of the MEXT (Notice No.71, 2006, MEXT, Japan). AQP4 null mice were generated as described previously (acc. No. CDB0758 K: http://www.cdb.riken.jp/arg/mutant%20mice%20list.html) [18]. For experiments in an inbred strain, the AQP4 null genotype was transferred to the Balb/cAJcl (CLEA Japan. Inc.) by >12 back-crosses.

2.2. Immunohistochemistry

Mice were anesthetized with isoflurane, and then perfused with saline followed by 4% paraformaldehyde in PBS. After mice were killed, TGs and DRGs were harvested, postfixed, and cryoprotected with 20% sucrose in PBS. Tissue sections were cryocut and incubated with 5% normal goat serum in 0.2% Triton X-100/PBS to block nonspecific binding. The sections were then incubated overnight with primary antibodies; anti-AQP4 (1:1000, made in rabbit, Sigma, MO, USA), anti-Kir4.1 (1:1000, made in rabbit, Alomone labs, Jerusalem, Israel), anti-AQP1 (1:1000, made in rabbit, Alpha Diagnostic, TX, USA), and Alexa 488- conjugated anti-NeuN (1:200, made in mouse, Millipore, CA, USA). The immunoreactivity was visualized using secondary antibodies conjugated to Alexa 488 or Alexa 555 (each 1:500; Invitrogen, CA, USA). To visualize nuclei, a mounting medium containing an instant-blue nuclear probe fluorescing compound (SouthernBiotech, AL, USA) was applied. Images were acquired using an inverted fluorescence microscope (Olympus, Tokyo, Japan). For some experiments, immunostained slices were observed with a confocal microscope (Olympus). DAB immunostaining was performed using EnVision systems (DAKO, CA, USA) as described previously [19]. Tissues were fixed with 5% paraformaldehyde, paraffin-embedded and sliced at 5 μm thickness. The sections were deparaffinized in xylene, rised in 100% and 70% ethanol, and blocked with 10% goat serum for 15 min at room temperature. The sections were then incubated with anti-AQP4 antibody (1:200, made in rabbit, Santa Cruz, Texas, USA) for 16 h at 4 °C. HRP-conjugated anti-rabbit IgG antibody was applied as a secondary antibody. The sections were counterstained with haematoxylin.

2.3. Western blotting

Two TGs, 20–30 DRGs from thoracic and lumber spinal cord and cerebellum from each mouse were homogenized in a homogenizing buffer [0.32 M sucrose, 10 mM HEPES (pH 7.4), 2 mM EDTA, protease inhibitors (cOmplete ULTRA Tablets, Mini, EDTA-free EASYpack, Roche, Mannheim, Germany), centrifuged at 1000×*g* for 15 min, and the supernatant was ultracentrifuged at 200,000×*g* for 1 h at 4 °C (Type SW 60 Ti rotor, Beckman Coulter, CA, USA) to obtain crude membrane pellets. Pellets were lysed in RIPA buffer [150 mM NaCl, 1.0% Triton X-100, 0.5% sodium deoxycholate, 0.1% SDS, 50 mM Tris (pH 8.0), and protease inhibitors (Roche)]. Total protein was measured using a BCA protein assay reagent kit (Pierce, IL, USA). Samples were incubated at 37 °C for 15 min in 5X Lammli sample buffer. The protein samples (50 μg for TG and DRG samples, 2 μg for cerebellum samples) were separated on a 12% SDS–PAGE and transferred onto a PVDF membrane, blocked with 5% skim milk in PBS, and incubated with a primary antibody against AQP4 (1:2000, made in rabbit, Sigma) overnight at 4 °C followed by the incubation with an HRP-conjugated secondary antibody (1:2000, Sigma) for 1 h at room temperature. Signals were visualized with a chemiluminescence (Immobilon western, Millipore) and detected with Image Quant LAS system (GE healthcare, WI, USA).

2.4. RT-PCR analysis

Cerebellum, spinal cord, DRGs and TGs were harvested from wild type and AQP4$^{-/-}$ mice after euthanasia and immediately homogenized in Isogen reagent (Wako, Osaka, Japan) for the isolation of total RNA. Reverse transcription reaction was performed using SuperScript® VILO™ Master Mix (Invitrogen). The resulting cDNA products were amplified by PCR using GoTaq® Green Master Mix (Promega, WI, USA). For PCR, we performed 30 cycles using the following conditions: 1 min at 94 °C, 1 min at 59 °C and 30 s at 72 °C. β-Actin was used as an internal control. The sequences of primers used in RT-PCR were as follows: for mouse AQP4: forward: 5′-CTTTCAAAGGAGTCTGGACTCAGGC-3′; reverse: 5′-CTTTCAAAGGAGTCTGGACTCAGGC-3′. For β-actin: forward: 5′-TGTATGCCTCTGGTCGTACC-3′; reverse: 5′-CAGGTCCAGACGCAGGATG-3′. PCR products (10 μl) were separated on 1% agarose gels with ethidium bromide and photographed under an ultraviolet illuminator.

2.5. Surgery

Spared nerve injury surgery was performed as described previously [20] under 3–5% sevoflurane (Maruishi, Osaka, Japan) anesthesia. The three branches of the sciatic nerve were exposed and both the tibial and common peroneal nerves were ligated and transected together, while the sural nerve was carefully preserved. The muscles and skin were then closed with a suture. The animals were recovered from the general anesthesia in a pre-warmed chamber, and housed as usual.

2.6. Assessment of mechanical and cold hypersensitivity

Each mouse was individually placed in an acryl cylinder on a wire mesh floor and habituated to the environment for 30 min prior to the testing. Mechanical sensitivity was measured with von Frey monofilaments perpendicularly applied to the lateral side of the plantar surface of the hindpaw. A positive response was noted if the paw was promptly withdrawn, flinched or licked. The 50% threshold of mechanical sensitivity was measured and calculated based on a up-and-down paradigm described as previously [21]. Sensitivity to cold stimuli was assessed with the acetone drop test [22]. One droplet of acetone was applied to the lateral side of the plantar surface of the hindpaw, and the duration of the nocifensive response (biting, licking, or shaking of paw) was measured over 30 s. The test was repeated 3 times to calculate the averages.

3. Results

To examine whether AQP4 is expressed in sensory ganglia, we first performed immunohistochemistry (IHC) for DRG and TG specimens from wild-type mice, using specimens from AQP4$^{-/-}$ mice as

negative controls. In the DRG and TG from wild-type mice, positive immunoreactivity was observed in regions of dense neuronal cell bodies, and not in areas containing bundles of sensory nerve fibers (Fig. 1A, B, left). No remarkable signals were seen in sensory ganglia from AQP4$^{-/-}$ mice (Fig. 1A, B, left). These findings suggest that the positive signals seen in the sensory ganglia from wild-type mice represent AQP4.

In higher magnification images, the AQP4 signals seemed to include small DAPI signals that are thought to represent the nuclei of satellite glial cells (SGCs) surrounding the neuronal cell bodies, suggesting that AQP4 is exclusively expressed in SGCs in sensory ganglia (Fig. 1A, B, right).

To confirm the localization of AQP4 in SGCs surrounding the neuronal cell bodies in sensory ganglia, we used a neuron-specific marker, NeuN. In both the DRG and the TG, the AQP4 signal did not overlap but precisely surrounded the neuronal cell bodies indicated by NeuN (Fig. 2A, B). This AQP4 staining pattern resembled that of Kir 4.1, a SGC-specific marker, and was totally distinct from that of AQP1, which is reportedly expressed only in neurons [6,10]. Furthermore, confocal microscopy analyses revealed that AQP4 signals were seen as double lines sandwiching the nuclear signals of SGCs, suggesting that AQP4 is expressed in both the inner and outer plasma membranes of SGCs (Fig. 2A, B, right).

The expression of AQP4 in sensory ganglia was further confirmed using biochemical analyses. In a Western blotting analysis, weak but distinct signals corresponding to AQP4 were observed in the membrane fractions of DRG and TG from wild-type mice, but not in those from AQP4$^{-/-}$ mice (Fig. 3A). AQP4 has two splicing isoforms: a full-length protein starting from Met1 (AQP4 M1), and an alternative shorter splicing isoform starting from Met23 (AQP4 M23). By comparing the band patterns for sensory ganglia and the cerebellum, the majority of AQP4 in the sensory ganglia seems to be the AQP4 M23 isoform. RT-PCR also confirmed the expression of AQP4 transcripts in DRG and TG from wild-type mice, but not in those from AQP4$^{-/-}$ mice (Fig. 3B). Compared with the strong signals in the cerebellum and spinal cord, in which AQP4 is abundantly expressed, the relatively weak AQP4 signals in the DRG and TG imply a relatively low AQP4 expression level in sensory ganglia.

Taking into account the expression of AQP4 in sensory ganglia, as well as in astrocytes in the CNS, it seems reasonable that AQP4 might play a role in the processing of sensory perception. To test this possibility, we examined the responsiveness to sensory stimuli by comparing wild-type and AQP4$^{-/-}$ mice. However, no significant differences in mechanical or cold sensitivity under either basal or neuropathic pain conditions were seen between wild-type and AQP4$^{-/-}$ mice, suggesting that the development of mechanical hypersensitivity and cold hypersensitivity in AQP4$^{-/-}$ mice did not differ from that in wild-type mice (Fig. 4A, B).

4. Discussion

In the present study, we identified the expression of AQP4 in sensory ganglia in the peripheral nervous system using immunohistochemistry and biochemical analyses of AQP4$^{-/-}$ mice as negative controls. Double immunostaining with a neuronal marker, NeuN, revealed that AQP4 is specifically expressed in SGCs surrounding neuronal cell bodies. To our knowledge, this is the first report demonstrating the presence of AQP4 in sensory ganglia in the peripheral nervous system (PNS).

In the CNS, AQP4 is specifically expressed in astrocytes, where it is localized to the foot processes at brain–water interfaces, such as perivascular endfeet, glia limiting membranes, and subependymal processes [7,8]. The osmotic-driven rapid water flux through astrocytic AQP4 may contribute to the maintenance of the ECS homeostasis in the CNS, in concert with other ion channels and neurotransmitter transporters expressed in astrocytes [23,24]. Likewise, SGCs in sensory ganglia contribute to the regulation of the ECS environment around sensory neurons through their expression of ion channels and transporters, such as Kir4.1 and EAAT [17]. Moreover, SGCs express dystrophin complex, which defines the localization of AQP4 to the perivascular endfeet of astrocytes through a protein–protein interaction [25]. Given these functional and structural similarities between astrocytes and SGCs, it seems reasonable that SGCs also express AQP4.

Our results demonstrated the expression of AQP4 in sensory ganglia, although the expression level is considerably lower than that in astrocytes. This difference might explain why the expression of AQP4 in sensory ganglia has attracted little attention to date. Indeed, to detect AQP4 expression in the DRG, 20–30 DRGs had to be collected and membrane fractionation using ultracentrifugation was required. In addition, SGCs have laminar structures and do not have any foot processes, as seen in astrocytes where AQP4 is highly enriched. This morphological difference may also contribute to the relatively lower expression of AQP4 in SGCs.

Although accumulating evidence suggests the involvement of AQP4 in sensory perception, the exact roles of AQP4 in sensory signal transduction remain elusive. Comparative studies using AQP4$^{-/-}$ mice revealed that AQP4 is expressed in supporting cells in the inner ear and that the genetic depletion of AQP4 results in abnormal auditory-evoked responses and hearing disturbances [10]. Subsequent studies also demonstrated the expression of AQP4 in the retina and olfactory epithelium, and AQP4$^{-/-}$ mice exhibit abnormalities in electroretinography and electro-olfactography [9,11]. Electrophysiological and computer simulation studies have suggested active roles of water flux through astrocytic AQP4 in K^+ buffering, working in concert with Kir4.1; in turn, these effects

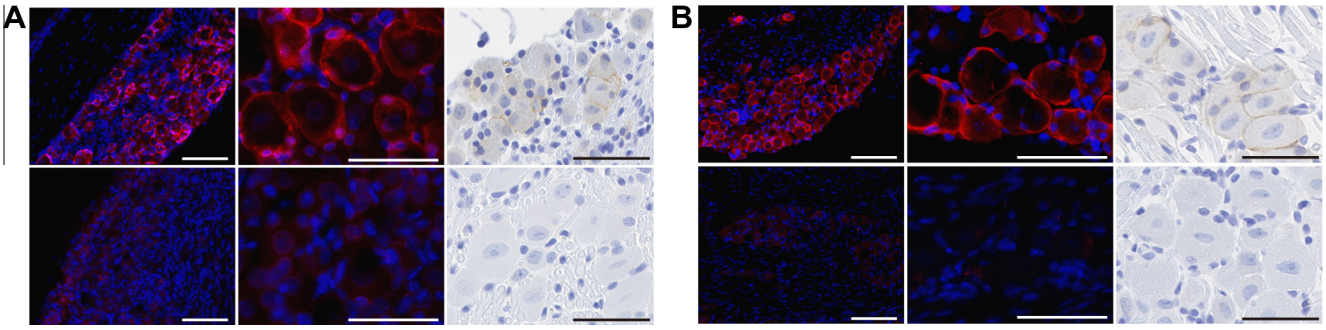

Fig. 1. AQP4 immunostaining in DRG (A) and TG (B) from wild-type (upper panels) and AQP4$^{-/-}$ mice (lower panels). AQP4 was labeled in red, and the nuclei were identified using DAPI (blue). Low (left, bar = 100 μm) and high (middle, bar = 50 μm) magnification images are shown. AQP4 immunoreactivity was not seen in sensory nerve axons (asterisks). Representative images of DAB staining for AQP4 in sensory ganglia are also shown (right, bar = 50 μm). (For interpretation of the references to colour in this figure legend, the reader is referred to the web version of this article.)

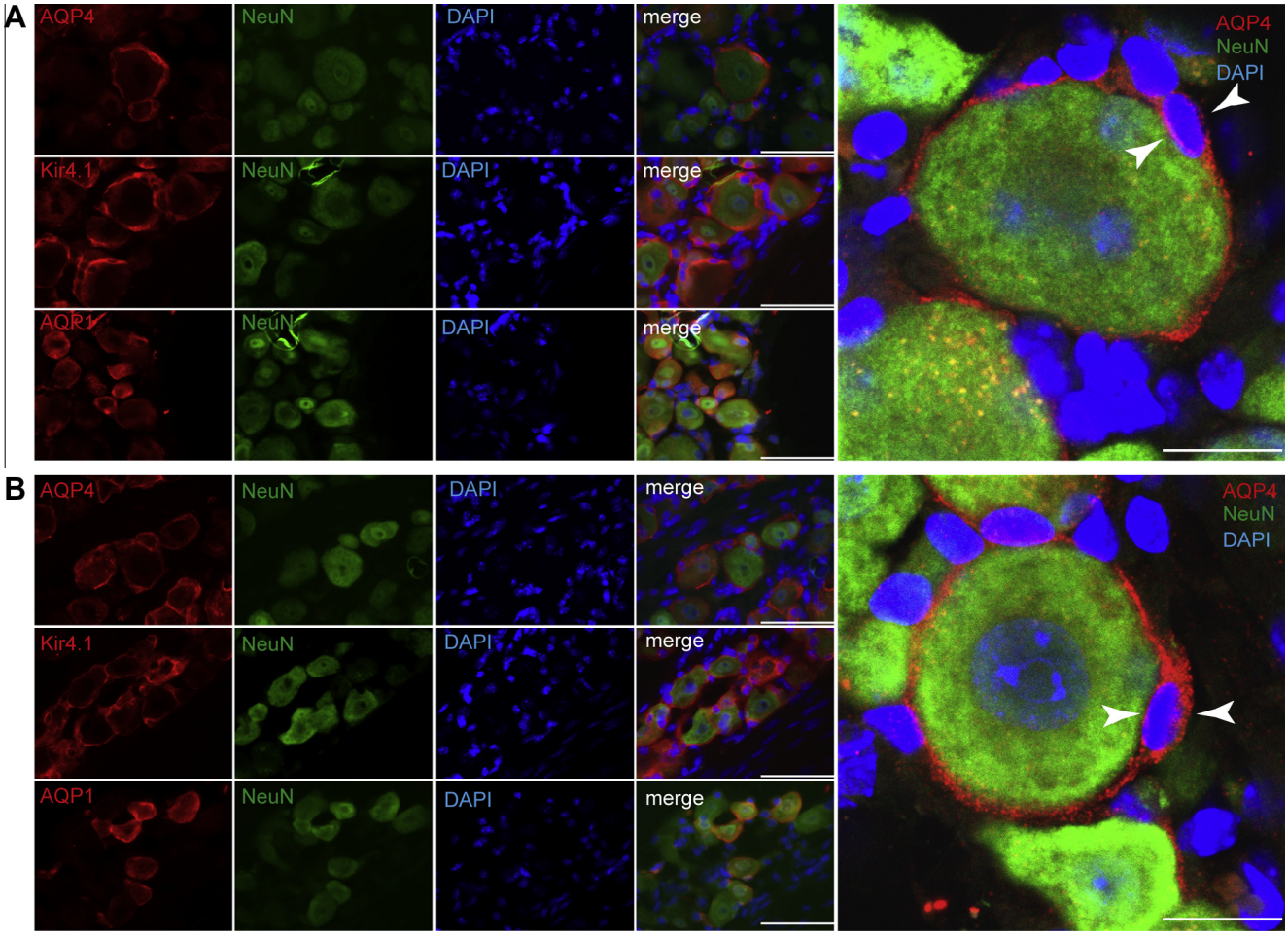

Fig. 2. Double immunostaining with NeuN (a neuronal marker) and AQP4, Kir4.1, or AQP1 in DRG (A) and TG (B) from wild-type mice. AQP4 (top), Kir4.1 (middle), and AQP1 (bottom) were labeled in red, NeuN was labeled in green, and the nuclei were identified using DAPI (blue). Laser confocal microscopic images of double staining with NeuN and AQP4 are also shown (right). AQP4 immunoreactivity sandwiched the nuclei of the SGCs (arrowheads). Bar = 50 μm. (For interpretation of the references to colour in this figure legend, the reader is referred to the web version of this article.)

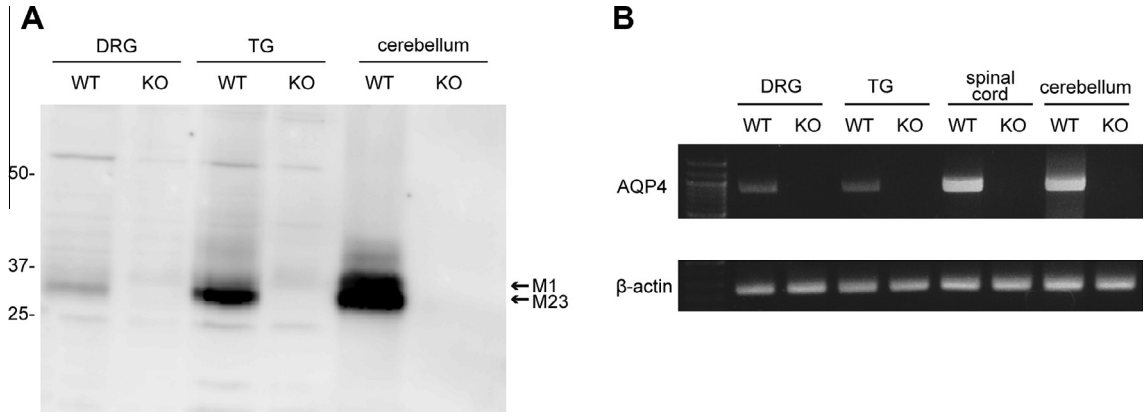

Fig. 3. (A) Western blot analysis for AQP4 expression in DRG and TG from wild-type and AQP4$^{-/-}$ mice. Cerebellum samples were used as controls. The molecular weights corresponding to the two AQP4 splicing isoforms are indicated as M1 and M23, respectively. (B) RT-PCR analysis for AQP4 transcript expression in DRG and TG from wild-type and AQP4$^{-/-}$ mice. Spinal cord and cerebellum samples are used as controls. No template control is also shown. β-Actin was used as an internal control.

influence neuronal excitability in the CNS [23,26]. Indeed, AQP4$^{-/-}$ mice showed delayed potassium clearance from the ECS around neurons and prolonged seizure activities in an epilepsy model [12]. These studies have highlighted the active involvement of AQP4 in the regulation of neuronal activities in the CNS. On the other hand, little attention has been paid regarding the involvement of AQP4 in peripheral somatosensory perception. SGCs also express Kir4.1 and contribute to the maintenance of electrolyte homeostasis in the ECS around the primary sensory neurons in sensory ganglia [17,27]; these actions are analogous to the homeostatic activities of astrocytes in the CNS. Therefore, the presence of AQP4 in SGCs should be advantageous.

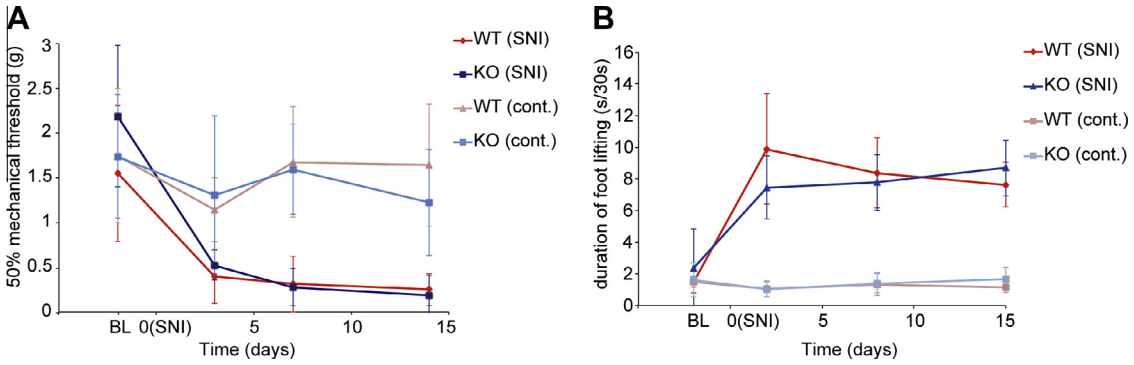

Fig. 4. Comparison of mechano-nociception and thermo-nociception between wild-type ($n = 6$) and AQP4$^{-/-}$ ($n = 6$) mice in a spared-nerve injury model. (A) Mechanical sensitivity was measured using an up-down method for obtaining the 50% threshold with von Frey hairs applied to the paw. (B) Thermal sensitivity was evaluated by cooling using an acetone droplet (approximately 10–15 °C) applied to the paw. The total durations of paw lifting over 30 s following the acetone application were measured. The results for the contralateral paw are also shown. The data are expressed as the mean ± SD.

In this study, we used a peripheral neuropathic pain model to explore the pathophysiological roles of AQP4 in peripheral somatosensory perception. Neuropathic pain is a pathological chronic pain condition in which peripheral nerve injury causes the disruption of electrolyte homeostasis in sensory ganglia, leading to neuronal hyper-excitability and abnormal firing [28–30]. This pathological condition is considered to be a peripheral form of epilepsy and, therefore, the involvement of AQP4 in its pathogenesis is highly likely. However, no remarkable differences in mechanical or thermal sensitivity were observed between wild-type and AQP4$^{-/-}$ mice under not only baseline conditions, but also under neuropathic pain conditions. One possible explanation is the lower expression level of AQP4 in sensory ganglia, as discussed above. The considerably low expression of AQP4 in sensory ganglia might imply a rudimentary expression as a result of evolutionary processes. Compensatory mechanisms by other aquaporins expressed in sensory ganglia, such as AQP1 and AQP2 expressed in sensory neurons [31,32], might be an alternative explanation. In contrast, another group has reported an altered nociceptive sensitivity using a formalin-induced acute pain model in AQP4$^{-/-}$ mice [33]. Further behavioral studies are needed to clarify the roles of AQP4 in peripheral somatosensory perception. Electrophysiological studies using sensory ganglia organ cultures could be helpful for examining the role of water flux through AQP4 expressed in SGCs in peripheral sensory perception.

Overall, we discovered the specific expression of AQP4 in SGCs in sensory ganglia in the PNS. Our findings provide novel insight into the involvement of water homeostasis in peripheral somatosensory perception.

Acknowledgments

We would like to thank Camilla Svensson and her colleagues for their kind technical support for the behavioral analyses and immunohistochemical analyses. The authors declare no conflicts of interests. This work was supported by the Keio Graduate School Doctral Student Grant-in-Aid Program (J.K.), Institutional Program for Young Researcher Overseas Visits from Japan Society for the Promotion of Science (J.K.), The Scandinavia-Japan Sasakawa Foundation (J.K.) and Keio University Program for the Advancement of Next Generation Research Projects (M.Y.), a Grant-in-Aid for Scientific Research on Innovative Areas for Glial assembly: a new regulatory machinery of brain function and disorders from the Ministry of Education, Culture, Sports, Science and Technology (MEXT), Japan (M.Y.).

Appendix A. Supplementary data

Supplementary data associated with this article can be found, in the online version, at http://dx.doi.org/10.1016/j.bbrc.2014.08.026.

References

[1] A. Frigeri, M.A. Gropper, F. Umenishi, M. Kawashima, D. Brown, A.S. Verkman, Localization of MIWC and GLIP water channel homologs in neuromuscular, epithelial and glandular tissues, J. Cell Sci. 108 (1995) 2993–3002.
[2] J.S. Jung, R.V. Bhat, G.M. Preston, W.B. Guggino, J.M. Baraban, P. Agre, Molecular characterization of an aquaporin cDNA from brain: candidate osmoreceptor and regulator of water balance, PNAS 91 (1994) 13052–13056.
[3] H. Hasegawa, M. Tonghui, W. Skach, A.M. Matthay, A.S. Verkman, Molecular cloning of a mercurial-insensitive water channel expressed in selected water-transporting tissues, J. Biol. Chem. 269 (1994) 5497–5500.
[4] K. Tani, T. Mitsuma, Y. Hiroaki, A. Kamegawa, K. Nishikawa, Y. Tanimura, et al., Mechanism of aquaporin-4's fast and highly selective water conduction and proton exclusion, J. Mol. Biol. 389 (2009) 694–706.
[5] Y. Cui, D.A. Bastien, Water transport in human aquaporin-4: molecular dynamics (MD) simulations, Biochem. Biophys. Res. Commun. 412 (2011) 654–659.
[6] M.C. Papadopoulos, A.S. Verkman, Aquaporin water channels in the nervous system, Nat. Rev. Neurosci. 14 (2013) 265–277.
[7] J. Rash, T. Yasumura, C. Hudson, P. Agre, S. Nielsen, Direct immunogold labeling of aquaporin-4 in square arrays of astrocyte and ependymocyte plasma membranes in rat brain and spinal cord, PNAS 95 (1998) 11981–11986.
[8] S. Nielsen, E.A. Nagelhus, M. Amiry-moghaddam, C. Bourque, P. Agre, O.P. Ottersen, Specialized membrane domains for water transport in glial cells : high-resolution immunogold cytochemistry of aquaporin-4 in rat brain, J. Neurosci. 17 (1997) 171–180.
[9] J. Li, R.V. Patil, A.S. Verkman, Mildly abnormal retinal function in transgenic mice without Müller cell aquaporin-4 water channels, Invest. Ophthalmol. Vis. Sci. 43 (2002) 573–579.
[10] J. Li, A.S. Verkman, Impaired hearing in mice lacking aquaporin-4 water channels, J. Biol. Chem. 276 (2001) 31233–31237.
[11] D.C. Lu, H. Zhang, Z. Zador, A.S. Verkman, Impaired olfaction in mice lacking aquaporin-4 water channels, FASEB J. 22 (2008) 3216–3223.
[12] D.K. Binder, X. Yao, Z. Zador, T.J. Sick, A.S. Verkman, Increased seizure duration and slowed potassium kinetics in mice lacking aquaporin-4 water channels, Glia. 53 (2006) 631–636.
[13] J. Kato, M.K. Hayashi, S. Aizu, Y. Yukutake, J. Takeda, M. Yasui, A general anaesthetic propofol inhibits aquaporin-4 in the presence of Zn^{2+}, Biochem. J. 454 (2013) 275–282.
[14] M.M. Thi, D.C. Spray, M. Hanani, Aquaporin-4 water channels in enteric neurons, J. Neurosci. Res. 86 (2008) 448–456.
[15] T. Ma, H. Gao, X. Fang, H. Yang, Expression and function of aquaporins in peripheral nervous system, Acta Pharmacol. Sin. 32 (2011) 711–715.
[16] H. Aldskogius, L.G. Elfvin, C.A. Forsman, Primary sensory afferents in the inferior mesenteric ganglion and related nerves of the guinea pig. An experimental study with anterogradely transported wheat germ agglutinin-horseradish peroxidase conjugate, J. Auton. Nerv. Syst. 15 (1986) 179–190.
[17] M. Hanani, Satellite glial cells in sensory ganglia: from form to function, Brain Res. Brain Res. Rev. 48 (2005) 457–476.
[18] H. Ikeshima-kataoka, Y. Abe, T. Abe, M. Yasui, Molecular and cellular neuroscience immunological function of aquaporin-4 in stab-wounded mouse brain in concert with a pro-inflammatory cytokine inducer, osteopontin, Mol. Cell. Neurosci. 56 (2013) 65–75.
[19] T. Misu, R. Höftberger, K. Fujihara, I. Wimmer, Y. Takai, S. Nishiyama, et al., Presence of six different lesion types suggests diverse mechanisms of tissue injury in neuromyelitis optica, Acta Neuropathol. 125 (2013) 815–827.
[20] A.F. Bourquin, M. Süveges, M. Pertin, N. Gilliard, S. Sardy, A.C. Davison, et al., Assessment and analysis of mechanical allodynia-like behavior induced by spared nerve injury (SNI) in the mouse, Pain 122 (14) (2006) e1–e14.
[21] S.R. Chaplan, F.W. Bach, J.W. Pogrel, J.M. Chung, T.L. Yaksh, Quantitative assessment of tactile allodynia in the rat paw, J. Neurosci. Methods 53 (1994) 55–63.

[22] S.B. Smith, S.E. Crager, J.S. Mogil, Paclitaxel-induced neuropathic hypersensitivity in mice: responses in 10 inbred mouse strains, Life Sci. 74 (2004) 2593–2604.
[23] N. MacAulay, T. Zeuthen, Water transport between CNS compartments: contributions of aquaporins and cotransporters, Neuroscience 168 (2010) 941–956.
[24] N. Macaulay, T. Zeuthen, Glial K^+ clearance and cell swelling: key roles for cotransporters and pumps, Neurochem. Res. 37 (2012) 2299–2309.
[25] K. Kamakura, Expression of dystroglycan complex in satellite cells of dorsal root ganglia, Acta Neuropathol. 101 (2001) 174–178.
[26] B.J. Jin, H. Zhang, D.K. Binder, A.S. Verkman, Aquaporin-4-dependent K(+) and water transport modeled in brain extracellular space following neuroexcitation, J. Gen. Physiol. 141 (2013) 119–132.
[27] H. Hibino, Y. Horio, A. Fujita, A.A. Inanobe, K. Doi, T. Gotow, et al., Expression of an inwardly rectifying K+ channel, Kir4.1, in satellite cells of rat cochlear ganglia, Am. J. Physiol. 277 (1999) C638–C644.
[28] R.D. Treede, T.S. Jensen, J.N. Campbell, G. Cruccu, J.O. Dostrovsky, J.W. Griffin, et al., Neuropathic pain: redefinition and a grading system for clinical and research purposes, Neurology 70 (2008) 1630–1635.
[29] H. Blumberg, W. Jänig, Discharge pattern of afferent fibers from a neuroma, Pain 20 (1984) 335–353.
[30] C. Liu, P.D. Wall, E. Bendor, M. Michaelis, R. Amir, M. Devor, Tactile allodynia in the absence of C-fiber activation: altered firing properties of DRG neurons following spinal nerve injury 85 (2000) 503–521.
[31] K. Oshio, H. Watanabe, D. Yan, A.S. Verkman, G.T. Manley, Impaired pain sensation in mice lacking Aquaporin-1 water channels, Biochem. Biophys. Res. Commun. 341 (2006) 1022–1028.
[32] B. Buffoli, E. Borsani, R. Rezzani, L.F. Rodella, Chronic constriction injury induces aquaporin-2 expression in the dorsal root ganglia of rats, J. Anat. 215 (2009) 498–505.
[33] F. Bao, M. Chen, Y. Zhang, Z. Zhao, Hypoalgesia in mice lacking aquaporin-4 water channels, Brain Res. Bull. 83 (2010) 298–303.